


## Article

# Novel Indane Derivatives with Antioxidant Activity from the Roots of *Anisodus tanguticus*

Chun-Wang Meng<sup>1,2,†</sup>, Hao-Yu Zhao<sup>1,2,†</sup>, Huan Zhu<sup>1,2</sup>, Cheng Peng<sup>1</sup>, Qin-Mei Zhou<sup>1,2,3,\*</sup> and Liang Xiong<sup>1,2,\*</sup>

<sup>1</sup> State Key Laboratory of Southwestern Chinese Medicine Resources, School of Pharmacy, Chengdu University of Traditional Chinese Medicine, Chengdu 611137, China

<sup>2</sup> Institute of Innovative Medicine Ingredients of Southwest Specialty Medicinal Materials, School of Pharmacy, Chengdu University of Traditional Chinese Medicine, Chengdu 611137, China

<sup>3</sup> Innovative Institute of Chinese Medicine and Pharmacy, Chengdu University of Traditional Chinese Medicine, Chengdu 611137, China

\* Correspondence: zhqmyx@sina.cn (Q.-M.Z.); xiling@cduetcm.edu.cn (L.X.)

† These authors contributed equally to this work.

**Abstract:** Four novel indane derivatives, anisotindans A–D (1–4), were isolated from the roots of *Anisodus tanguticus*. Their structures were established using comprehensive spectroscopic analyses, and their absolute configurations were determined by electronic circular dichroism (ECD) calculations and single-crystal X-ray diffraction analyses. Anisotindans C and D (3 and 4) are two unusual indenofuran analogs. ABTS<sup>•+</sup> and DPPH<sup>•+</sup> assays of radical scavenging activity reveal that all compounds (1–4) are active. Specifically, the ABTS<sup>•+</sup> assay results show that anisotindan A (1) exhibits the best antioxidant activity with an IC<sub>50</sub> value of 15.62 ± 1.85 μM (vitamin C, IC<sub>50</sub> = 22.54 ± 5.18 μM).

**Keywords:** *Anisodus tanguticus*; indanes; indenofuran; absolute configuration; antioxidant activity



**Citation:** Meng, C.-W.; Zhao, H.-Y.; Zhu, H.; Peng, C.; Zhou, Q.-M.; Xiong, L. Novel Indane Derivatives with Antioxidant Activity from the Roots of *Anisodus tanguticus*.

*Molecules* **2023**, *28*, 1493. <https://doi.org/10.3390/molecules28031493>

Academic Editors: Iryna Smetanska and Oksana Sytar

Received: 2 January 2023

Revised: 26 January 2023

Accepted: 31 January 2023

Published: 3 February 2023



**Copyright:** © 2023 by the authors. Licensee MDPI, Basel, Switzerland. This article is an open access article distributed under the terms and conditions of the Creative Commons Attribution (CC BY) license (<https://creativecommons.org/licenses/by/4.0/>).

## 1. Introduction

*Anisodus tanguticus* (Maxim.) Pascher is a folk medicine commonly used in northwest and southwest China [1,2]. The roots of *A. tanguticus* can relieve pain and spasms, promote blood circulation, remove blood stasis, stop bleeding, and strengthen muscles. Moreover, they are often used in the clinical treatment of pain, ulcer, colitis, gallstone, traumatic injury, catagma, hemorrhage, anesthesia, and motion sickness [3–5]. Due to its scarce plant resources, wild *A. tanguticus* was once listed as a class II protected endangered plant in the List of National Key Protected Wild Plants (the first batch). However, the implementation of long-term environmental protection strategies and the establishment of several planting bases in Ganzi and Aba (Sichuan Province) have significantly improved the plant resources of this species over the past years. Today, *A. tanguticus* is considered an important economic plant due to its high content of tropane-type alkaloids. Moreover, this plant is currently the natural resource of anisodamine, anisodine, hyoscyne, and cuscohygrine.

In light of their significant biological activities, such as anti-shock effect [6], amelioration of hypoxic injury [7], cardioprotective effect [8], and alleviation of angina symptoms [9], the tropane-type alkaloids in *A. tanguticus* have been extensively researched. However, few studies are available on the non-alkaloid components of the plant. Previously, we had isolated a series of compounds from *A. tanguticus*, including four new sesquiterpenoids with an unprecedented skeleton [10,11]. In this study, four novel indane derivatives (1–4) were isolated (Figure 1). Indanes are generally characterized by anti-tumor [12], anti-microbial [13–15], anti-inflammatory [16,17], neuroprotective [18], and antioxidant activities [19], and, thus, they have been used to develop various drugs, such as indacaterol, aprindine, and donepezil. Knowing that indanes have significant free radical scavenging activity [19], the scavenging activity of compounds 1–4 is analyzed herein using ABTS<sup>•+</sup> and DPPH<sup>•+</sup> assays.

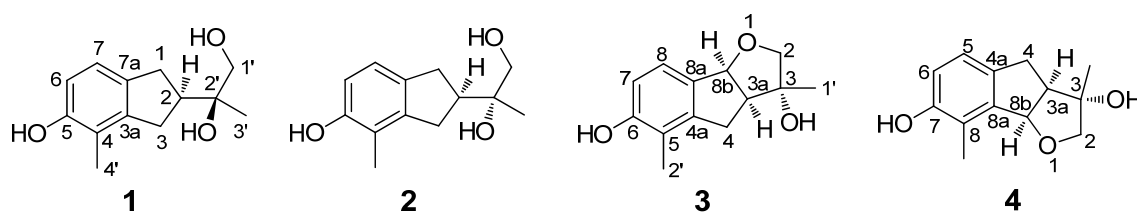


Figure 1. Structures of the novel indanes (1–4) isolated from *A. tanguticus*.

## 2. Results

### 2.1. Structure Elucidation

Anisotindan A (**1**) was obtained as colorless crystals, and based on HR-ESI-MS analysis, its molecular formula is  $C_{13}H_{18}O_3$ , with five degrees of unsaturation ( $m/z$  245.1157, calcd. for  $C_{13}H_{18}O_3Na$ , 245.1154). The  $^1H$  NMR spectrum of **1** displays signals corresponding to *ortho*-coupled aromatic protons [ $\delta_H$  6.77 (1H, d,  $J = 8.4$  Hz) and 6.59 (1H, d,  $J = 8.4$  Hz)], an oxymethylene group [ $\delta_H$  3.48 (1H, dd,  $J = 10.8, 6.0$  Hz) and 3.45 (1H, dd,  $J = 10.8, 6.0$  Hz)], two aliphatic methylene groups [ $\delta_H$  2.91 (1H, dd,  $J = 15.0, 9.0$  Hz), 2.76 (1H, dd,  $J = 15.0, 9.0$  Hz), and 2.82 (2H, m)], one aliphatic methine group [ $\delta_H$  2.65 (1H, m)], two tertiary methyl groups [ $\delta_H$  2.09 (3H, s) and 1.19 (3H, s)], and three exchangeable protons [ $\delta_H$  7.77 (1H, s), 3.70 (1H, t,  $J = 6.0$  Hz), and 3.28 (1H, s)]. The  $^{13}C$  NMR and DEPT spectra exhibit carbon resonance signals that can be assigned to the protonated units listed above, as well as to five quaternary carbons ( $\delta_C$  154.4, 144.3, 134.7, 120.4, and 73.7). Comprehensive 2D NMR analysis reveals  $^1H$ - $^1H$  COSY correlations of  $H_{2-1}/H_{2-3}$  and  $H_{6-7}$ , in conjunction with HMBC correlations of  $H_{2-1}$  with C-3, C-3a, C-7, and C-7a, and of  $H_{2-3}$  with C-3a and C-4 in the indane framework of **1** (Figure 2). Based on the HMBC correlations from  $H_{2-1}$  and  $H_{2-3}$  to C-2'; from H-2 to C-1', C-2', and C-3'; from  $H_{2-1'}$  to C-2, C-2', and C-3'; from  $H_{3-3'}$  to C-2, C-1', and C-2'; from OH-2' to C-2, C-2', and C-3'; and from OH-1' to C-1' and C-2', as well as the  $^1H$ - $^1H$  COSY correlation of  $H_{2-1'}/OH-1'$ , a 1,2-dihydroxyisopropyl unit is established at C-2. The HMBC correlations of  $H_{3-4'}$  with C-3a, C-4, and C-5, and of OH-5 with C-4, C-5, and C-6 indicate that a methyl group and a hydroxy group are substituted at C-4 and C-5, respectively. Finally, single-crystal X-ray crystallography analysis [Flack parameter = 0.02(13)] reveals that the absolute configuration of **1** is 2*R*,2'*S* (Figure 3).

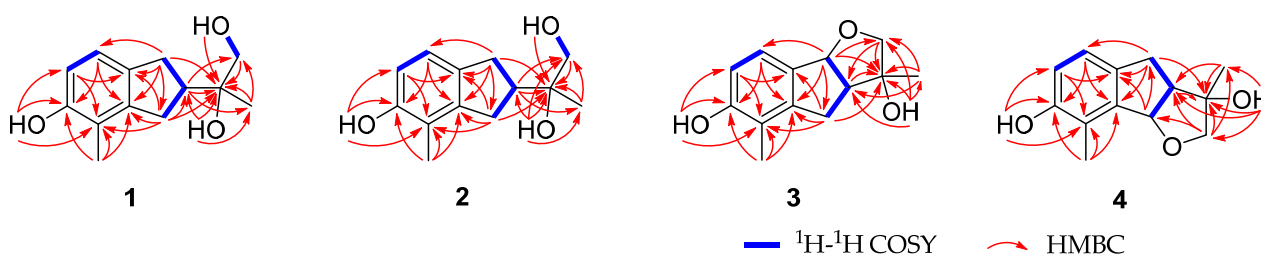


Figure 2. Key  $^1H$ - $^1H$  COSY and HMBC correlations of compounds 1–4.

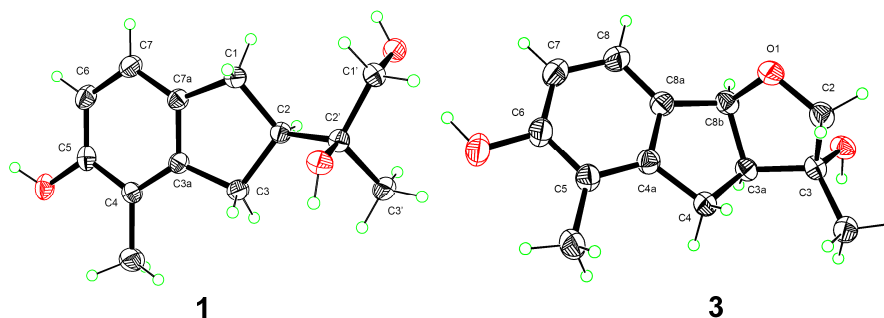


Figure 3. X-ray crystallographic structures of compounds 1 and 3.

Anisotindan B (**2**) was obtained as a white powder, and its molecular formula was found to be  $C_{13}H_{18}O_3$ , the same as **1**. As shown in Table 1, the  $^1H$  and  $^{13}C$  NMR data of **2** are highly similar to those of **1**, which suggests that the former might be an epimer of the latter. This is further confirmed by 2D NMR analysis (HSQC,  $^1H$ - $^1H$  COSY, and HMBC). Thus, compound **2** may be identified as (2*S*,2'*S*)-**2** or its enantiomer. A comparison of the calculated and experimental ECD data (Figure 4) reveals that the absolute configuration of compound **2** is 2*R*,2'*R*.

**Table 1.**  $^1H$  and  $^{13}C$  NMR data for compounds **1–4** in acetone- $d_6$  ( $\delta$  in ppm,  $J$  in Hz).

No.	1 <sup>a</sup>		2 <sup>a</sup>		3 <sup>b</sup>		4 <sup>b</sup>	
	$\delta_H$	$\delta_C$	$\delta_H$	$\delta_C$	$\delta_H$	$\delta_C$	$\delta_H$	$\delta_C$
1	2.91 dd (15.0, 9.0) 2.76 dd (15.0, 9.0)	33.5	2.82 dd (15.0, 9.0) 2.78 dd (15.0, 9.0)	34.1				
2	2.65 m	47.5	2.66 m	47.5	3.58 dd (8.4, 0.7) 3.36 d (8.4)	77.9	3.61 dd (9.1, 0.7) 3.37 d (9.1)	78.1
3	2.82 m	33.4	2.84 overlapped	32.8		80.5		80.4
3a		144.3		144.7	2.91 m	55.5	2.91 overlapped	55.4
4		120.4		120.5	2.95 dd (15.4, 9.1) 2.73 dd (15.4, 4.2)	33.3	2.91 overlapped 2.76 dd (20.3, 9.8)	33.8
4a						145.1		134.7
5		154.4		154.4		120.1	6.81 d (7.7)	122.5
6	6.59 d (8.4)	113.6	6.59 d (8.4)	113.6		156.5	6.74 d (7.7)	116.6
7	6.77 d (8.4)	122.2	6.78 d (8.4)	122.2	6.70 d (8.4)	114.7		155.0
7a		134.7		134.4				
8					6.97 d (8.4)	123.9		122.3
8a						134.1		143.3
8b					5.47 d (6.3)	88.1	5.61 d (6.3)	87.2
1'	3.48 dd (10.8, 6.0) 3.45 dd (10.8, 6.0)	69.8	3.49 dd (10.2, 6.0) 3.46 dd (10.2, 6.0)	69.9	1.32 s	20.9	1.30 s	20.7
2'		73.7		73.7	2.09 s	12.1	2.22 s	12.0
3'	1.19 s	22.9	1.17 s	22.8				
4'	2.09 s	12.4	2.09 s	12.4				
OH-3					3.83 s		3.87 s	
OH-5	7.77 s		7.76 s					
OH-6					8.10 s			
OH-7							7.92 s	
OH-1'	3.70 t (6.0)		3.71 t (6.0)					
OH-2'	3.28 s		3.29 s					

<sup>a</sup> Data were measured at 600 MHz for  $^1H$  and 150 MHz for  $^{13}C$ . <sup>b</sup> Data were measured at 700 MHz for  $^1H$  and 175 MHz for  $^{13}C$ .

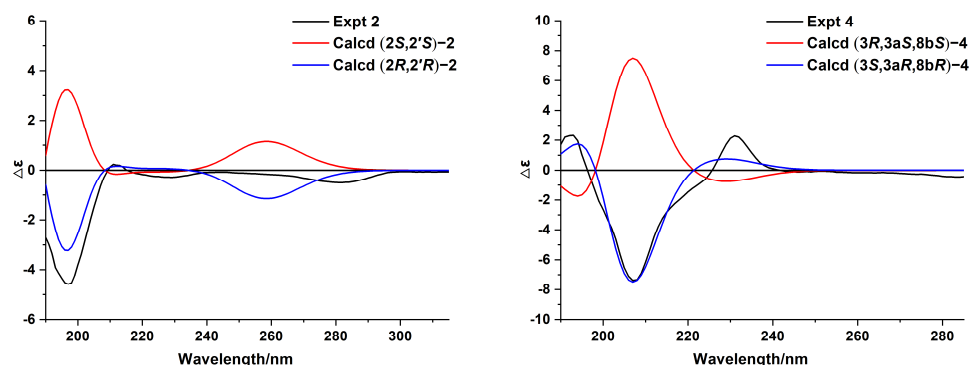


**Figure 4.** Experimental and calculated ECD spectra of compounds **2** and **4**.

Anisotindan C (**3**) was obtained as colorless crystals, and it has the molecular formula  $C_{13}H_{16}O_3$ , with six degrees of unsaturation (two fewer protons than compounds **1** and **2**), as evidenced by HR-ESI-MS analysis ( $m/z$  243.0996, calcd. for  $C_{13}H_{16}O_3Na$ , 243.0997). The  $^1H$  and  $^{13}C$  NMR spectra of compound **3** suggest that this compound is an analog of compound **2**. Indeed, comparison of the NMR data corresponding to the two compounds reveals that a methylene group in **2** is replaced by an oxymethine group [ $\delta_H$  5.47 (1H, d,  $J$  = 6.3 Hz),  $\delta_C$

88.1] in compound **3**. In addition, the signal of the exchangeable hydrogen proton (OH-1') is observed in the  $^1\text{H}$  NMR spectrum of compound **2**, but not in the spectrum of **3**. This indicates that compound **3** is an ether derivative of compound **2**. The 2D NMR spectra of compound **3** confirmed its planar structure, especially the HMBC correlation of H-8b to C-2 (Figure 2). Moreover, H-3a, H-8b, and OH-3 in **3** have the same orientation, as evidenced by the enhancement of H-3a and OH-3 signals upon the irradiation of H-8b in 1D NOE spectroscopy analysis. The small coupling constant between H-3a and H-8b ( $J_{3a,8b} = 6.3$  Hz) also indicates that H-3a and H-8b are *cis* oriented [20]. Single-crystal X-ray diffraction analysis [Flack coefficient 0.08(7)] (Figure 3) shows that the absolute configuration of **3** is 3*R*,3*aS*,8*bS*.

Anisotindan D (**4**) is an isomer of compound **3**, as indicated by HR-ESI-MS,  $^1\text{H}$ , and  $^{13}\text{C}$  NMR data. Comparison of the  $^1\text{H}$  and  $^{13}\text{C}$  NMR spectra of the two compounds reveals that the compound **4** is an isomer of compound **3**. As shown in Figure 2, the  $^1\text{H}$ - $^1\text{H}$  COSY and HMBC correlations reveal the presence of the 3,3*a*,4,8*b*-tetrahydro-2*H*-indeno [1,2-*b*]furan skeleton. In addition, the HMBC correlations of OH-3 with C-2, C-3, and C-1'; OH-7 with C-6, C-7, and C-8; and of H<sub>3</sub>-2' with C-7, C-8, and C-8*a* confirm that two hydroxy groups and a methyl group are substituted at C-3, C-7, and C-8, respectively. Based on the NOE correlations of H-8b with H-3a and OH-3, as well as the small coupling constant between H-3a and H-8b ( $J_{3a,8b} = 6.3$  Hz), H-3a, H-8b, and OH-3 in **4** have the same orientation. As shown in Figure 4, the calculated ECD spectrum of (3*S*,3*aR*,8*bR*)-**4** is consistent with the experimental spectrum, and thus, the absolute configuration of compound **4** is 3*S*,3*aR*,8*bR*.

## 2.2. Antioxidant Activities

As shown in Table 2, compounds **1**, **2**, **3**, and **4** exhibit ABTS free radical scavenging activities, with IC<sub>50</sub> values of  $15.62 \pm 1.85$ ,  $40.92 \pm 7.02$ ,  $43.93 \pm 9.35$ , and  $32.38 \pm 6.29$   $\mu\text{M}$ , respectively. The activity of compound **1**, the most potent scavenger, is even stronger than that of vitamin C (VC, IC<sub>50</sub> =  $22.54 \pm 5.18$   $\mu\text{M}$ ). Based on the DPPH<sup>•+</sup> assay, compound **1** also has an antioxidant effect, with an IC<sub>50</sub> value of  $68.46 \pm 17.34$   $\mu\text{M}$ . However, the remaining compounds do not exhibit antioxidant activity, even at concentrations as high as 100  $\mu\text{M}$ . Interestingly, the antioxidant activities of epimers **1** and **2** are quite different, despite the similar structures of the two compounds (differ only in the absolute configuration of C-2').

**Table 2.** ABTS<sup>•+</sup> and DPPH<sup>•+</sup> scavenging activities of compounds 1–4 <sup>a</sup>.

	IC <sub>50</sub> for ABTS <sup>•+</sup> Scavenging Assay ( $\mu\text{M}$ )	IC <sub>50</sub> for DPPH <sup>•+</sup> Scavenging Assay ( $\mu\text{M}$ )
<b>1</b>	$15.62 \pm 1.85$	$68.46 \pm 17.34$
<b>2</b>	$40.92 \pm 7.02$	>100
<b>3</b>	$43.93 \pm 9.35$	>100
<b>4</b>	$32.38 \pm 6.29$	>100
VC	$22.54 \pm 5.18$	$10.19 \pm 1.38$

<sup>a</sup> All values are represented as Mean  $\pm$  SD,  $n = 3$ .

## 3. Discussion

Indanes are a class of small organic molecules with a benzocyclopentane skeleton that can be substituted with 4-aminobenzylidene, gallic acid, piperidine, cyclohexadienone, or nucleobase to form indane analogs with diverse structures and significant activity [21]. Many reports are available in the literature regarding the synthesis of indane analogs via Friedel–Crafts-type, Michael-type, and Heck-type cyclization reactions [21,22]. However, reports on naturally occurring indanes are scarce. Notably, *A. tanguticus* seems to contain several indane derivatives, including rare polyhydroxy indenofurans.

Oxidative stress, a condition induced by the excessive generation of free radicals, is considered to be an important cause of human disease and aging. Indeed, the accumulation of reactive species in cells can lead to DNA damage, as well as protein and lipid degrada-

tion, which affects normal physiological functions [23]. Therefore, antioxidants play an important role in the prevention and treatment of diseases, and their development has attracted increasing attention [24–26]. Knowing that polyhydroxy compounds are potent antioxidants, and that they are widely present in plants [27,28], this study investigates the polyhydroxy (two or three hydroxy groups) indane derivatives in *A. tanguticus*. In total, four novel compounds are isolated, and their antioxidant activities are evaluated using ABTS<sup>•+</sup> and DPPH<sup>•+</sup> assays. The obtained results reveal that all four indane derivatives (1–4) identified herein have good free radical scavenger activities, with 1 being the most active compound. Comparison of the structures of compounds 1–4 suggests that the strong activity of compound 1 may be attributed to the OH-1' substitution and the configuration of C-2'. However, ABTS<sup>•+</sup> and DPPH<sup>•+</sup> assays are just simplified methods for estimating antioxidant activity, which do not reflect the actual antioxidant activity [29]. Unfortunately, further studies on the antioxidant activity of compounds 1–4 could not be carried out due to their limited sample quantities.

Indene analogs generally have significant neuroprotective effects [21]. Indeed, donepezil, a second-generation AChE inhibitor, is used to treat Alzheimer's disease due to its significant cholinesterase inhibitory activity. In light of this information, as well as the strong AChE inhibitory effect of the *A. tanguticus* extract [30], the AChE inhibitory activity of the compounds isolated herein is also analyzed in this study using the modified Ellman method [31] and donepezil as a positive control. However, none of the compounds show inhibitory activity against AChE, even at concentrations as high as 100 µM.

## 4. Materials and Methods

### 4.1. General Experimental Procedures

Optical rotation was measured using a Rudolph Autopol I automatic polarimeter (Rudolph Research Analytical, Hackettstown, NJ, USA). ECD and IR spectra were recorded on an Applied Photophysics Chirascan CD spectrometer (Applied Photophysics Ltd., Leatherhead, UK) and an Agilent Cary 600 FT-IR microscope instrument (Agilent Technologies Inc., Santa Clara, CA, USA), respectively. X-ray crystallographic analyses were performed on a Bruker D8 Quest diffractometer (Bruker Corporation, Billerica, MA, USA). Meanwhile, NMR and HR-ESI-MS spectra were acquired on a Bruker Avance NEO 600 or a Bruker Avance NEO 700 spectrometer (solvent peaks used as the references) and a Waters Synapt G2 HDMS (Waters Corporation, Milford, MA, USA) or a Bruker timsTOF MS instrument, respectively. The melting points were measured on a BÜCHI M-565 melting point apparatus (BÜCHI Labortechnik AG, Flawil, Switzerland). MPLC separations were carried out using a BÜCHI Pure C-805 instrument. HPLC separations were performed on an Agilent 1220 instrument with a Welch Ultimate XB-C<sub>18</sub> column (10 × 250 mm<sup>2</sup>, 5 µm) or a Daicel Chiralpak AD-H column (4.6 × 250 mm<sup>2</sup>, 5 µm). TLC was carried out using silica gel GF254 plates (Anhui Liangchen Silicon Material Co. Ltd., Lu'an, Anhui, China), whereas column chromatography separations were performed on silica gel (200–300 mesh, Yantai Institute of Chemical Technology, Yantai, Shandong, China), Sephadex LH-20 (40–70 µm, Amersham Pharmacia Biotech AB, Uppsala, Sweden), or ODS (40 µm, Acchrom Technology Co. Ltd., Beijing, China).

### 4.2. Plant Material

The roots of *A. tanguticus* (Maxim.) Pascher (Solanaceae) were collected from Aba Tibetan and Qiang Autonomous Prefecture in Sichuan Province, China, during the month of October in 2017. The collected samples were identified by Dr. Ji-hai Gao (Chengdu University of TCM, Chengdu, Sichuan, China) and deposited at Chengdu No. 1 Pharmaceutical Co. Ltd. in Chengdu, Sichuan, China.

### 4.3. Extraction and Isolation

The powdered roots of *A. tanguticus* (500 kg) were dampened with ammonia, and then extracted with diethoxymethane (6 × 500 L) under countercurrent extraction for 2 h at room

temperature. The extracting solution was partitioned with 20% sulfuric acid, affording aqueous and organic phases. The organic phase was concentrated under reduced pressure to yield a residue (3 kg). Part of the residue (1 kg) was suspended in H<sub>2</sub>O and successively partitioned with petroleum ether and EtOAc. The EtOAc fraction (60 g) was subjected to silica gel column chromatography and eluted with petroleum ether–EtOAc (50:1–1:1) and EtOAc–MeOH (1:0–0:1) to afford 9 fractions (Fr.1–Fr.9). Among them, Fr.7 (17.9 g) was chromatographed over a Sephadex LH-20 column (petroleum ether–CH<sub>2</sub>Cl<sub>2</sub>–MeOH, 5:5:1) to give 12 subfractions (Fr.7-1–Fr.7-12). Subfraction Fr.7-11 (2.8 g) was separated into six subfractions (Fr.7-11-1–Fr.7-11-6) on a Sephadex LH-20 column (MeOH–H<sub>2</sub>O, 80:20). Subsequently, subfraction Fr.7-11-4 (153 mg) was separated by silica gel chromatography (CH<sub>2</sub>Cl<sub>2</sub>–Me<sub>2</sub>CO, 20:1–1:1) and reverse-phase semi-preparative HPLC (40% MeOH in H<sub>2</sub>O) into several mixtures, including a mixture of compound 3 and 4 (9 mg, t<sub>R</sub> = 28.7 min). The pure compounds were chirally separated on a Daicel Chiralpak AD-H column using normal-phase HPLC (*n*-hexane/ethanol, 5:1). Compound 3 (4 mg) was eluted at 9.5 min, whereas compound 4 (4 mg) was eluted at 14.3 min. Fr.7-12 (500 mg) was first separated by silica gel column chromatography into five subfractions (Fr.7-12-1–Fr.7-12-5), using CH<sub>2</sub>Cl<sub>2</sub>–MeOH (100:1–10:1) as the mobile phase. Thereafter, Fr.7-12-1 (150 mg) was purified by preparative TLC (CH<sub>2</sub>Cl<sub>2</sub>–MeOH, 17:1) and reverse-phase semi-preparative HPLC (50% MeOH in H<sub>2</sub>O), followed by normal-phase HPLC (*n*-hexane/ethanol, 3:1) to afford compounds 1 (5 mg, t<sub>R</sub> = 11.8 min) and 2 (2 mg, t<sub>R</sub> = 6.5 min).

#### 4.4. Physicochemical Properties and Spectroscopic Data of Compounds 1–4

Anisotindan A [(2*R*)-5-Hydroxy-4-methyl-2-((2*S*)-1,2-dihydroxyisopropyl)indane] (1): colorless crystals; mp 174–176 °C;  $[\alpha]_D^{20}$  –17.0 (*c* 0.02, MeOH); UV (MeCN)  $\lambda_{\max}$  (log  $\epsilon$ ) 282 (2.89), 218 (3.57), 199 (4.32) nm; ECD (MeCN) 194 ( $\Delta\epsilon$  –3.15), 283 ( $\Delta\epsilon$  –0.24) nm; IR  $\nu_{\max}$  3358, 2922, 2852, 1658, 1634, 1604, 1541, 1470, 1384, 1263, 1049, 1031, 940, 862, 807 cm<sup>–1</sup>; <sup>1</sup>H NMR (acetone-*d*<sub>6</sub>, 600 MHz) and <sup>13</sup>C NMR (acetone-*d*<sub>6</sub>, 150 MHz) data, see Table 1; (+)-HR-ESI-MS *m/z* 245.1157 [M + Na]<sup>+</sup> (calcd. for C<sub>13</sub>H<sub>18</sub>O<sub>3</sub>Na, 245.1154). The original UV, IR, (+)-HR-ESI-MS, <sup>1</sup>H NMR, <sup>13</sup>C NMR, DEPT, HSQC, <sup>1</sup>H-<sup>1</sup>H COSY, and HMBC spectra are shown in Figures S3–S11, Supplementary Material.

Anisotindan B [(2*R*)-5-Hydroxy-4-methyl-2-((2*R*)-1,2-dihydroxyisopropyl)indane] (2): white powder;  $[\alpha]_D^{20}$  –15.0 (*c* 0.02, MeOH); UV (MeCN)  $\lambda_{\max}$  (log  $\epsilon$ ) 283 (2.96), 218 (3.65), 199 (4.47) nm; ECD (MeCN) 197 ( $\Delta\epsilon$  –4.58), 282 ( $\Delta\epsilon$  –0.50) nm; IR  $\nu_{\max}$  3424, 2935, 2850, 1659, 1631, 1603, 1455, 1349, 1266, 1160, 1071, 1027, 940, 811 cm<sup>–1</sup>; <sup>1</sup>H NMR (acetone-*d*<sub>6</sub>, 600 MHz) and <sup>13</sup>C NMR (acetone-*d*<sub>6</sub>, 150 MHz) data, see Table 1; (+)-HR-ESI-MS *m/z* 245.1148 [M + Na]<sup>+</sup> (calcd. for C<sub>13</sub>H<sub>18</sub>O<sub>3</sub>Na, 245.1154). The original UV, IR, (+)-HR-ESI-MS, <sup>1</sup>H NMR, <sup>13</sup>C NMR, DEPT, HSQC, <sup>1</sup>H-<sup>1</sup>H COSY, and HMBC spectra are shown in Figures S12–S20, Supplementary Material.

Anisotindan C [(3*R*,3*aS*,8*bS*)-3,6-Dihydroxy-3,5-dimethyl-3,3*a*,4,8*b*-tetrahydro-2*H*-indeno[1,2-*b*]furan] (3): colorless crystals; mp 209–211 °C;  $[\alpha]_D^{20}$  +19.0 (*c* 0.03, MeOH); UV (MeCN)  $\lambda_{\max}$  (log  $\epsilon$ ) 279 (2.83), 221 (3.70), 200 (4.54) nm; ECD (MeCN) 191 ( $\Delta\epsilon$  –4.19), 204 ( $\Delta\epsilon$  0.55), 209 ( $\Delta\epsilon$  –0.97), 230 ( $\Delta\epsilon$  2.49) nm; IR  $\nu_{\max}$  3357, 3278, 2921, 2850, 1659, 1633, 1603, 1470, 1426, 1383, 1353, 1271, 1243, 1152, 1132, 1024, 970, 934, 893, 816, 754, 705 cm<sup>–1</sup>; <sup>1</sup>H NMR (acetone-*d*<sub>6</sub>, 700 MHz) and <sup>13</sup>C NMR (acetone-*d*<sub>6</sub>, 175 MHz) data, see Table 1; (+)-HR-ESI-MS *m/z* 243.0996 [M + Na]<sup>+</sup> (calcd. for C<sub>13</sub>H<sub>16</sub>O<sub>3</sub>Na, 243.0997). The original UV, IR, (+)-HR-ESI-MS, <sup>1</sup>H NMR, <sup>13</sup>C NMR, DEPT, HSQC, <sup>1</sup>H-<sup>1</sup>H COSY, HMBC, and 1D NOE spectra are shown in Figures S21–S30, Supplementary Material.

Anisotindan D [(3*S*,3*aR*,8*bR*)-3,7-Dihydroxy-3,8-dimethyl-3,3*a*,4,8*b*-tetrahydro-2*H*-indeno[1,2-*b*]furan] (4): white powder;  $[\alpha]_D^{20}$  –53.0 (*c* 0.05, MeOH); UV (MeCN)  $\lambda_{\max}$  (log  $\epsilon$ ) 285 (3.28), 218 (3.86), 199 (4.58) nm; ECD (MeCN) 193 ( $\Delta\epsilon$  2.32), 207 ( $\Delta\epsilon$  –7.37), 231 ( $\Delta\epsilon$  2.28) nm; IR  $\nu_{\max}$  3356, 3270, 2921, 2851, 1659, 1633, 1498, 1469, 1429, 1382, 1333, 1266, 1180, 1051, 1023, 974, 919, 882, 815, 717, 707 cm<sup>–1</sup>; <sup>1</sup>H NMR (acetone-*d*<sub>6</sub>, 700 MHz) and <sup>13</sup>C NMR (acetone-*d*<sub>6</sub>, 175 MHz) data, see Table 1; (+)-HR-ESI-MS *m/z* 243.0997 [M + Na]<sup>+</sup> (calcd. for C<sub>13</sub>H<sub>16</sub>O<sub>3</sub>Na, 243.0997). The original UV, IR, (+)-HR-ESI-MS, <sup>1</sup>H NMR, <sup>13</sup>C NMR,

DEPT, HSQC,  $^1\text{H}$ - $^1\text{H}$  COSY, HMBC, and 1D NOE spectra are shown in Figures S31–S40, Supplementary Material.

#### 4.5. X-ray Crystallographic Data of Compounds 1 and 3

Crystals of **1** and **3** were obtained from MeOH. Intensity data were collected on a Bruker D8 Quest diffractometer equipped with an APEX-II CCD using Cu K $\alpha$  radiation. Crystallographic data for the reported structures have been deposited at the Cambridge Crystallographic Data Centre (CCDC). Copies of the data can be acquired free of charge from CCDC, 12 Union Road, Cambridge CB2 1EZ, UK (fax: +44-1223-336-033; e-mail: deposit@ccdc.cam.ac.uk).

Crystal data for **1**:  $\text{C}_{13}\text{H}_{18}\text{O}_3$ ,  $M = 222.27$ , colorless crystals, monoclinic,  $a = 6.7889(2)$  Å,  $b = 8.5863(2)$  Å,  $c = 10.5065(3)$  Å,  $a = 90^\circ$ ,  $\beta = 106.502(1)^\circ$ ,  $\gamma = 90^\circ$ ,  $V = 587.21(3)$  Å $^3$ , space group  $P2_1$ ,  $T = 293(2)$  K,  $Z = 2$ ,  $\mu(\text{Cu K}\alpha) = 0.713$  mm $^{-1}$ , 10,969 reflections measured, 2125 independent reflections ( $R_{\text{int}} = 0.0395$ ). Final  $R$  indices ( $I > 2\sigma(I)$ ):  $R_1 = 0.0344$ ,  $wR_2 = 0.0810$ . Final  $R$  indices (all data):  $R_1 = 0.0385$ ,  $wR_2 = 0.0844$ . The goodness of fit on  $F^2$  was 1.093. Flack parameter = 0.02(13). CCDC number: 2232633.

Crystal data for **3**:  $\text{C}_{13}\text{H}_{16}\text{O}_3$ ,  $M = 220.26$ , colorless crystals, orthorhombic,  $a = 6.156(3)$  Å,  $b = 9.879(4)$  Å,  $c = 18.688(9)$  Å,  $a = 90^\circ$ ,  $\beta = 90^\circ$ ,  $\gamma = 90^\circ$ ,  $V = 1136.4(9)$  Å $^3$ , space group  $P2_12_12_1$ ,  $T = 273(2)$  K,  $Z = 4$ ,  $\mu(\text{Cu K}\alpha) = 0.736$  mm $^{-1}$ , 41,583 reflections measured, 2086 independent reflections ( $R_{\text{int}} = 0.0513$ ). Final  $R$  indices ( $I > 2\sigma(I)$ ):  $R_1 = 0.0347$ ,  $wR_2 = 0.0924$ . Final  $R$  indices (all data):  $R_1 = 0.0367$ ,  $wR_2 = 0.0951$ . The goodness of fit on  $F^2$  was 1.056. Flack parameter = 0.08(7). CCDC number: 2232632.

#### 4.6. ECD Calculation

The details of ECD calculation of compounds **2** and **4** are shown in Texts S1 and S2, Figures S1 and S2, and Tables S1 and S2, Supplementary Material.

#### 4.7. Antioxidant Activity

The ABTS and DPPH free radical scavenging assays were used to estimate the antioxidant activities of the isolated compounds.

##### 4.7.1. ABTS $\bullet^+$ Assay

The free radical scavenging capacity of compounds **1–4** was measured using the ABTS $\bullet^+$  decoloration method. First, 20 mL ABTS $\bullet^+$  solution (7 mM) and 20 mL of potassium persulfate solution (2.45 mM) were prepared with ultra-pure water. The prepared solutions were mixed and stored in the dark at 23 °C for 16 h to obtain ABTS $\bullet^+$  stock solution. Two milliliters of this solution were subsequently diluted (20 times) with 95% ethanol solution to obtain the ABTS $\bullet^+$  working solution with an absorbance of  $0.70 \pm 0.02$  at 734 nm. Thereafter, compound solutions (80  $\mu\text{L}$ ) of varying concentrations were mixed with 400  $\mu\text{L}$  of the ABTS $\bullet^+$  working solution and added into 96-well plates, with 150  $\mu\text{L}$  in each well. After 6 min incubation in the dark at 23 °C, the absorbance (OD) of each sample was measured at 734 nm. Using vitamin C as the positive control and 95% ethanol solution as the blank control, the scavenging rate of ABTS free radicals was calculated according to the following equation: (%) =  $(1 - A_s/A_c) \times 100\%$ , where  $A_s$  and  $A_c$  are the average OD values of the drug group and the blank control group, respectively. All tests were performed in triplicate.

##### 4.7.2. DPPH $\bullet^+$ Assay

DPPH $\bullet^+$  solution (0.1 mM) was prepared with 95% ethanol, and 250  $\mu\text{L}$  of the solution was mixed with compound solutions (250  $\mu\text{L}$ ) of varying concentrations. The mixtures were transferred into 96-well plates, with 150  $\mu\text{L}$  in each well. After the reaction at 25 °C for 30 min, the absorbance (OD) was measured at 517 nm, and the DPPH free radical scavenging rate was calculated according to the following equation: (%) =  $(1 - A_s/A_c) \times 100\%$ ,

where  $A_s$  and  $A_c$  are the average OD values of the drug group and the blank control group (95% ethanol solution), respectively. All tests were performed in triplicate.

## 5. Conclusions

In this study, four new indanes (1–4), anisotindans A–D, were extracted from the roots of *A. tanguticus*. Their structures were identified by NMR and single-crystal X-ray crystallography analyses, as well as ECD calculations. Meanwhile, their antioxidant activity was estimated using ABTS and DPPH free radical scavenging assays. The obtained results show that anisotindans C and D (3 and 4) are two unusual indenofuran analogs, and that compounds 1–4 exhibit significant antioxidant capacity, especially compound 1, the ABTS radical scavenging capacity of which is greater than that of vitamin C. The preliminary structure–activity relationship analysis conducted herein suggests that the variation in antioxidant activity of indanes may be attributed to differences in OH-1' substitution and C-2' configuration.

**Supplementary Materials:** The following supporting information can be downloaded at: <https://www.mdpi.com/xxx/s1>, Figures S1 and S2 are the optimized conformers of (2S,2'S)-2 and (3R,3aS,8bS)-4; Figures S3–S40 are UV, IR, HR-ESI-MS, 1D NMR, and 2D NMR spectra of compounds 1–4; Table S1. Energy analysis for the conformers of (2S,2'S)-2; Table S2. Energy analysis for the conformers of (3R,3aS,8bS)-4; Text S1 and S2 are the ECD calculation of compounds 2 and 4 [32–36].

**Author Contributions:** C.-W.M. and H.-Y.Z. performed most of the phytochemical experiments and wrote the manuscript, and both authors contributed equally to this work. H.Z. helped to complete the phytochemical experiments. C.P., Q.-M.Z. and L.X. conceived the project and designed the experiments. L.X. revised the manuscript. All authors have read and agreed to the published version of the manuscript.

**Funding:** This work was supported by the National Natural Science Foundation of China (Grant No. 82022072), the Innovation Team and Talents Cultivation Program of the National Administration of Traditional Chinese Medicine (Grant No. ZYYCXTD-D-202209), and the “Xinglin Scholar” Plan of Chengdu University of Traditional Chinese Medicine (Grant No. XKTD2022006).

**Institutional Review Board Statement:** Not applicable.

**Informed Consent Statement:** Not applicable.

**Data Availability Statement:** The data presented in this study are available in the Supplementary Materials or can be provided by the authors.

**Conflicts of Interest:** The authors declare no conflict of interest.

**Sample Availability:** Samples of the compounds are available from the authors.

## References

1. Zang, E.H.; Li, Q.Y.; Xu, J.F.; Zhang, Y.; Jiang, L.L.; Li, X.; Zhang, M.X.; Liu, Y.C.; Wu, Q.J.; Liu, Z.H.; et al. A preliminary pharmacophylogenetic study of Solanaceae medicinal plants containing tropane alkaloids. *China J. Chin. Mater. Med.* **2021**, *46*, 4344–4359. [[CrossRef](#)]
2. Wang, Y.; Guo, Z.; Hu, G.; Li, G.; Niu, S.; Zhao, F. Separation, identification and pesticidal activity of alkaloids from *Anisodus tanguticus* (Maxim.) Pascher. *Plant Prot.* **2019**, *45*, 190–194. [[CrossRef](#)]
3. Ma, L.; Gu, R.; Tang, L.; Chen, Z.E.; Di, R.; Long, C. Important poisonous plants in Tibetan ethnomedicine. *Toxins* **2015**, *7*, 138–155. [[CrossRef](#)] [[PubMed](#)]
4. Zhang, X.F.; Wang, H. The variation of the contents of four tropane alkaloids in *Anisodus tanguticus*. *Acta Bot. Boreali-Occident. Sin.* **2002**, *22*, 630–634. [[CrossRef](#)]
5. Huang, J.P.; Wang, Y.J.; Tian, T.; Wang, L.; Yan, Y.; Huang, S.X. Tropane alkaloid biosynthesis: A centennial review. *Nat. Prod. Rep.* **2021**, *38*, 1634–1658. [[CrossRef](#)] [[PubMed](#)]
6. Zhao, T.; Li, D.J.; Liu, C.; Su, D.F.; Shen, F.M. Beneficial effects of anisodamine in shock involved cholinergic anti-inflammatory pathway. *Front. Pharmacol.* **2011**, *2*, 23. [[CrossRef](#)] [[PubMed](#)]
7. Wang, J.; Zhu, Q.; Duan, X.; Li, L.; Zhang, S.; Chen, J.; Wang, Y. Evaluation of anisodamine-mediated amelioration of hypoxic injury in brain microvascular endothelial cells. *Trop. J. Pharm. Res.* **2022**, *20*, 1425–1432. [[CrossRef](#)]



8. Xing, K.; Fu, X.; Jiang, L.; Wang, Y.; Li, W.; Gu, X.; Hao, G.; Miao, Q.; Ge, X.; Peng, Y.; et al. Cardioprotective effect of anisodamine against myocardial ischemia injury and its influence on cardiomyocytes apoptosis. *Cell Biochem. Biophys.* **2015**, *73*, 707–716. [[CrossRef](#)]
9. Chen, L.; Lei, B.; Lou, Y.; Chen, L.; Jiang, J. Impact of intravenous administration of anisodamine on coronary microvascular dysfunction in patients with obstructive epicardial coronary artery disease after percutaneous coronary intervention. *Trop. J. Pharm. Res.* **2022**, *21*, 1045–1053. [[CrossRef](#)]
10. Zhao, H.Y.; Liu, J.; Zhu, H.; Liu, F.; Liu, Z.H.; Peng, C.; Xiong, L. New amides from the roots of *Anisodus tanguticus*. *Biochem. Syst. Ecol.* **2020**, *91*, 104082. [[CrossRef](#)]
11. Zhao, H.Y.; Zhou, Q.M.; Zhu, H.; Zhou, F.; Meng, C.W.; Shu, H.Z.; Liu, Z.H.; Peng, C.; Xiong, L. Anisotanols A–D, four norsesquiterpenoids with an unprecedented sesquiterpenoid skeleton from *Anisodus anguinus*. *Chin. J. Chem.* **2021**, *39*, 3375–3380. [[CrossRef](#)]
12. Singh, A.; Fatima, K.; Singh, A.; Behl, A.; Minto, M.J.; Hasanain, M.; Ashraf, R.; Luqman, S.; Shanker, K.; Mondhe, D.M.; et al. Anticancer activity and toxicity profiles of 2-benzylidene indanone lead molecule. *Eur. J. Pharm. Sci.* **2015**, *76*, 57–67. [[CrossRef](#)]
13. Almansour, A.I.; Ali, S.; Ali, M.A.; Ismail, R.; Choon, T.S.; Sellappan, V.; Elumalai, K.K.; Pandian, S. A regio- and stereoselective 1,3-dipolar cycloaddition for the synthesis of new-fangled dispiropyrrrolothiazoles as antimycobacterial agents. *Bioorg. Med. Chem. Lett.* **2012**, *22*, 7418–7421. [[CrossRef](#)] [[PubMed](#)]
14. Caputto, M.E.; Ciccarelli, A.; Frank, F.; Moglioni, A.G.; Moltrasio, G.Y.; Vega, D.; Lombardo, E.; Finkielstein, L.M. Synthesis and biological evaluation of some novel 1-indanone thiazolyldiazone derivatives as anti-Trypanosoma cruzi agents. *Eur. J. Med. Chem.* **2012**, *55*, 155–163. [[CrossRef](#)]
15. Mor, S.; Pahal, P.; Narasimhan, B. Synthesis, characterization, antimicrobial activities and QSAR studies of some 10a-phenylbenzo[b]indeno[1,2-e][1,4]thiazin-11(10aH)-ones. *Eur. J. Med. Chem.* **2012**, *53*, 176–189. [[CrossRef](#)]
16. Huang, H.C.; Chamberlain, T.S.; Selbert, K.; Koboldt, C.M.; Isakson, P.C.; Reitz, D.B. Diaryl indenenes and benzofurans: Novel classes of potent and selective cyclooxygenase-2 inhibitors. *Bioorg. Med. Chem. Lett.* **1995**, *5*, 2377–2380. [[CrossRef](#)]
17. Singh, P.; Prasher, P.; Dhillon, P.; Bhatti, R. Indole based peptidomimetics as anti-inflammatory and anti-hyperalgesic agents: Dual inhibition of 5-LOX and COX-2 enzymes. *Eur. J. Med. Chem.* **2015**, *97*, 104–123. [[CrossRef](#)]
18. Cacabelos, R. Pharmacogenetic considerations when prescribing cholinesterase inhibitors for the treatment of Alzheimer’s disease. *Expert Opin. Drug Metab. Toxicol.* **2020**, *16*, 673–701. [[CrossRef](#)]
19. Shin-Ya, K.; Furihata, K.; Teshima, Y.; Hayakawa, Y.; Seto, H. Structures of stealthins A and B, new free radical scavengers of microbial origin. *Tetrahedron Lett.* **1992**, *33*, 7025–7028. [[CrossRef](#)]
20. Ueno, K.; Furumoto, T.; Umeda, S.; Mizutani, M.; Takikawa, H.; Batchvarova, R.; Sugimoto, Y. Heliolactone, a non-sesquiterpene lactone germination stimulant for root parasitic weeds from sunflower. *Phytochemistry* **2014**, *108*, 122–128. [[CrossRef](#)]
21. Prasher, P.; Sharma, M. Medicinal chemistry of indane and its analogues: A mini review. *ChemistrySelect* **2021**, *6*, 2658–2677. [[CrossRef](#)]
22. Gabriele, B.; Mancuso, R.; Veltri, L. Recent advances in the synthesis of indanes and indenenes. *Chemistry* **2016**, *22*, 5056–5094. [[CrossRef](#)]
23. Guo, C.; Sun, L.; Chen, X.; Zhang, D. Oxidative stress, mitochondrial damage and neurodegenerative diseases. *Neural Regen. Res.* **2013**, *8*, 2003–2014. [[CrossRef](#)]
24. Wootton-Beard, P.C.; Ryan, L. Improving public health?: The role of antioxidant-rich fruit and vegetable beverages. *Food Res. Int.* **2011**, *44*, 3135–3148. [[CrossRef](#)]
25. Ratnam, D.V.; Ankola, D.D.; Bhardwaj, V.; Sahana, D.K.; Kumar, M.N. Role of antioxidants in prophylaxis and therapy: A pharmaceutical perspective. *J. Control. Release* **2006**, *113*, 189–207. [[CrossRef](#)]
26. Helberg, J.; Pratt, D.A. Autoxidation vs. antioxidants—The fight for forever. *Chem. Soc. Rev.* **2021**, *50*, 7343–7358. [[CrossRef](#)]
27. Evans, K.O.; Harry-O’kuru, R.E. Antioxidation behavior of milkweed oil 4-hydroxy-3-methoxycinnamate esters in phospholipid bilayers. *J. Am. Oil Chem. Soc.* **2013**, *90*, 1719–1727. [[CrossRef](#)]
28. Agnihotri, V.K.; Elsohly, H.N.; Khan, S.I.; Smillie, T.J.; Khan, I.A.; Walker, L.A. Antioxidant constituents of *Nymphaea caerulea* flowers. *Phytochemistry* **2008**, *69*, 2061–2066. [[CrossRef](#)] [[PubMed](#)]
29. Amorati, R.; Valgimigli, L. Advantages and limitations of common testing methods for antioxidants. *Free Radic. Res.* **2015**, *49*, 633–649. [[CrossRef](#)]
30. Yang, Z.D.; Ren, J.; Xue, P.H.; Yang, M.J. Screening of total alkaloids from Tibetan medicine for acetylcholinesterase inhibitory activity. *Chin. J. Exp. Tradit. Med. Formulae* **2011**, *17*, 194–196. [[CrossRef](#)]
31. Ellman, G.L.; Courtney, K.D.; Andres Jr., V.; Featherstone, R.M. A new and rapid colorimetric determination of acetylcholinesterase activity. *Biochem. Pharmacol.* **1961**, *7*, 88–95. [[CrossRef](#)] [[PubMed](#)]
32. Goto, H.; Osawa, E. Corner flapping: A simple and fast algorithm for exhaustive generation of ring conformations. *J. Am. Chem. Soc.* **1989**, *111*, 8950–8951. [[CrossRef](#)]
33. Goto, H.; Osawa, E. An efficient algorithm for searching low-energy conformers of cyclic and acyclic molecules. *J. Chem. Soc. Perkin Trans.* **1993**, *2*, 187–198. [[CrossRef](#)]
34. Frisch, M.J.; Trucks, G.W.; Schlegel, H.B.; Scuseria, G.E.; Robb, M.A.; Cheeseman, J.R.; Scalmani, G.; Barone, V.; Petersson, G.A.; Nakatsuji, H.; et al. *Gaussian 16*; Revision B.01; Gaussian, Inc.: Wallingford, CT, USA, 2016.

35. Liu, Y.; Liu, F.; Qiao, M.M.; Guo, L.; Chen, M.H.; Peng, C.; Xiong, L. Curcumanes A and B, two bicyclic sesquiterpenoids with significant vasorelaxant activity from *Curcuma longa*. *Org. Lett.* **2019**, *21*, 1197–1201. [[CrossRef](#)] [[PubMed](#)]
36. Bruhn, T.; Schaumlöffel, A.; Hemberger, Y.; Bringmann, G. *Spec Dis*, version 1.7; University of Würzburg: Würzburg, Germany, 2017.

**Disclaimer/Publisher's Note:** The statements, opinions and data contained in all publications are solely those of the individual author(s) and contributor(s) and not of MDPI and/or the editor(s). MDPI and/or the editor(s) disclaim responsibility for any injury to people or property resulting from any ideas, methods, instructions or products referred to in the content.